BJR

Received: 26 July 2013 | Revised: 29 October 2013 | Accepted: 8 November 2013

doi: 10.1259/bjr.20130464

Cite this article as:
Fraioli F, Punwani S. Clinical and research applications of simultaneous positron emission tomography and MRI. Br J Radiol 2014;87:20130464.

REVIEW ARTICLE

Clinical and research applications of simultaneous positron emission tomography and MRI

[1,2]F FRAIOLI, FRCR and [2,3]S PUNWANI, FRCR, PhD

[1]Institute of Nuclear Medicine, University College London, London, UK
[2]Division of Imaging, University College London Hospital, London, UK
[3]Centre for Medical Imaging, University College London, London, UK

Address correspondence to: Dr Shonit Punwani
E-mail: *shonit.punwani@gmail.com*

ABSTRACT

Evaluation of the molecular processes responsible for disease pathogenesis and progression represents the new frontier of clinical radiology. Multimodality imaging lies at the cutting edge, combining the power of MRI for tissue characterization, microstructural appraisal and functional assessment together with new positron emission tomography (PET) tracers designed to target specific metabolic processes. The recent commercial availability of an integrated clinical whole-body PET-MRI provides a hybrid platform for exploring and exploiting the synergies of multimodal imaging. First experiences on the clinical and research application of hybrid PET-MRI are emerging. This article reviews the rapidly evolving field and speculates on the potential future direction.

Recently, there has been significant interest in multimodal imaging with positron emission tomography (PET) and MRI in an attempt to exploit synergies between the two techniques. Software fusion of images acquired using separate PET and MRI machines has been most widely reported.[1,2] In response, manufacturers have integrated PET and MRI hardware.[3,4] Two options currently exist for those in the PET-MRI market: (i) the first involves two separate machines, with both machines being housed either in the same room or in adjacent rooms and fusion software used to combine sequentially acquired PET and MR images;[5,6] (ii) the second option integrates the PET detectors within the centre of an MR scanner, enabling simultaneous acquisition of signals from both modalities[7] (from here on referred to as simultaneous PET-MRI).

Simultaneous PET-MRI was initially developed for brain imaging using an MR-compatible PET insert placed within the bore of a conventional MRI scanner. The fused images overlay metabolic signals from PET on the high-resolution/soft-tissue contrast MR images, thereby providing improved localization of metabolic changes for a number of different clinical applications.[8–11]

More recently, Siemens AG® (Biograph mMR, Erlangen, Germany) has released the first whole-body simultaneous PET-MRI option for the clinical market. Comprising a 60-cm-bore 3-T magnet with an integrated ring of solid-state PET scintillation avalanche photodiode detectors insensitive to magnetic fields, the scanner is able to simultaneously acquire PET and MRI signals. This article reviews the potential clinical and research application of simultaneous PET-MRI for assessment of neurological, body oncological, cardiovascular and inflammatory diseases.

STRATEGIES FOR SIMULTANEOUS POSITRON EMISSION TOMOGRAPHY-MRI

There are several levels of complexity to which a simultaneous PET-MRI protocol can be developed.

Positron emission tomography with anatomical MRI for localization and attenuation correction

At the most basic level, a non-contrast anatomical MRI pulse sequence (*e.g.* T_2 or T_1 weighted imaging, Dixon, short tau–inversion–recovery etc.) can be acquired whilst PET signal is simultaneously collected at each bed position. In this case, the primary role of MRI is to replace the anatomical localization provided by the CT component of a PET-CT study. However, substituting MRI for CT is more challenging than it might first appear.

Firstly, CT provides electron density data necessary for attenuation correction of PET images. Indeed, for MRI to replace CT, it must also provide a measure of electron density; a capability that it does not have. Therefore,

an alternative approach is necessary. For the Siemens simultaneous PET-MRI, attenuation correction is based on Dixon fat and water separation sequences. Dixon[12] published the first paper on a simple water and fat separation in 1984. The technique he described acquires two separate images: the first, a conventional spin echo image with water and fat signals in phase and the other acquired with the readout gradient slightly shifted, so that the water and fat signals are 180° out of phase; the signals from the two allow derivation of separate fat and water images.[13] Attenuation correction of PET signal can be approximated by segmenting fat and water and assigning an assumed electron density to each component. However, a major limitation of this approach is in separating air from bone, as both generate no signal on Dixon images and yet have very different electron densities. Thus, accurate attenuation correction on PET-MRI remains a work in progress with a focus on improving Dixon techniques, whilst also exploring alternative strategies, *e.g.* attenuation maps and ultrashort echo time imaging.[7,14–18]

Secondly, it would not be correct to assume that the anatomical quality of MRI is equivalent to CT in all areas of the body; for example, CT has a significant advantage when imaging the lung and is also less prone to motion artefact within the abdomen. However, whether these advantages of CT are crucial to interpretation or whether the PET signal by itself can compensate for potentially reduced anatomical resolution and increased imaging artefact of MRI remains to be determined.

Positron emission tomography with diagnostic MRI

An alternative PET-MRI strategy combines diagnostic standalone MRI protocols with PET, bringing together two examinations into a single study whilst avoiding the radiation exposure associated with CT. This significantly increases the complexity of a PET-MRI study; a combined protocol has to be thought through to minimize patient scan time, whilst maintaining the diagnostic quality of MRI study. At this stage, it is not clear whether a full diagnostic MRI is necessary for any given examination; for example, it is not known whether gadolinium contrast will provide any additional benefit for lesion localization/characterization compared with an injected PET tracer.[19] Development of dedicated protocols for specific clinical indications will be a slow process, with each application necessitating individualized tailored protocols.

Positron emission tomography with multiparametric MRI for advanced tissue characterization

A third approach being trialled predominantly within the research arena is to combine the tissue characterization afforded by multiparametric MRI with signal from specific PET tracers. Multiparametric MRI has been successfully applied for imaging of local tumour sites, *e.g.* the prostate for localization of cancer foci,[20,21] and generally involves a combination of anatomical, diffusion-weighted and dynamic contrast-enhanced imaging to facilitate characterization of tissue fat/water content, cellularity and vascularity. The role of individual MRI sequences and their correlative/synergistic role with signals from ^{18}F-fludeoxyglucose (^{18}F-FDG) and other PET tracers remain to be explored.

NEUROLOGICAL APPLICATIONS OF POSITRON EMISSION TOMOGRAPHY-MRI

Brain imaging was one of the first applications for simultaneous PET-MRI systems,[22] as the anatomical site is less prone to patient motion. There is a growing interest within the neurological community in the application and development of novel radiopharmaceutical tracers for the evaluation of neurodegenerative and oncological disease with PET-MRI.

Alzheimer's disease

Dementia has been recognized as a growing problem for society in the UK. Alzheimer's disease (AD) is the leading cause of dementia in elderly adults, and its incidence worldwide is increasing.[23,24] Clinically, AD is characterized by progressive memory loss and impairment of other cognitive functions that significantly impair activities of daily living. The neuropathological hallmarks of AD include extracellular beta-amyloid (Aβ) deposition in the form of senile plaques and intracellular accumulation of neurofibrillary tangles (tau proteins), which induce a series of toxic events that lead to synaptic dysfunction, neuronal loss and brain atrophy.[25] Accumulation of amyloid occurs decades before the cognitive decline begins and has been proposed as the first step in a cascade of changes.

There are an increasing number of candidate drugs for the treatment of AD; these may have application for treatment of early-stage disease (*i.e.* before the cognitive impairment is apparent). PET-MRI is uniquely positioned to play a role in the assessment of novel drug treatments in longitudinal clinical trials and potentially the clinical diagnostic pathway.

^{18}F-FDG-PET can be used to measure the cerebral metabolic rate of glucose, an index of brain synaptic activity. Several ^{18}F-FDG-PET studies have been performed to qualitatively and quantitatively estimate AD-related brain changes.[26,27] These studies consistently show widespread metabolic deficits in the neocortical association areas, with sparing of the thalamus, basal ganglia, cerebellum, primary sensory motor cortex and visual cortex. Specifically, the so-called "AD metabolic pattern" is characterized by hypometabolism in associative parietotemporal areas, posterior cingulate cortex and precuneus, as well as medial temporal lobes, mostly entorhinal cortex and hippocampus (Figure 1). With advancing disease, hypometabolism extends to prefrontal cortex. Indeed, ^{18}F-FDG-PET has been demonstrated as a sensitive measure of longitudinal changes in brain glucose metabolism and proposed as a marker of disease progression and therapeutic response.[28,29]

A specific tracer with high affinity to amyloid plaques [thioflavin T compound also commercially named Pittsburgh compound B (PiB)] has been developed in the past decade. This compound has been labelled initially with ^{11}C (^{11}C-PiB).[30] Unfortunately, the short half-life of ^{11}C does not allow its use in centres without onsite tracer production facilities. In 2008, the thioflavin molecule was labelled with a fluorine compound, enabling its use within centres without cyclotrons.[31] Results from large multicentre trials have demonstrated high levels of cortical ^{11}C-PiB primarily involving the frontal, temporal and parietal association cortices of AD patients.[32] Furthermore, cortical ^{11}C-PiB levels have been correlated with increased cerebrospinal fluid (CSF)

Figure 1. Images of a 77-year-old male with cognitive impairment. MR shows volume loss, subarachnoid space dilatation and atrophy mainly in parietotemporal areas (arrow), medial temporal lobes, precuneus and hippocampi. Simultaneous ^{18}F-fludeoxyglucose-positron emission tomography demonstrates agreement between MR changes and areas of hypometabolism.

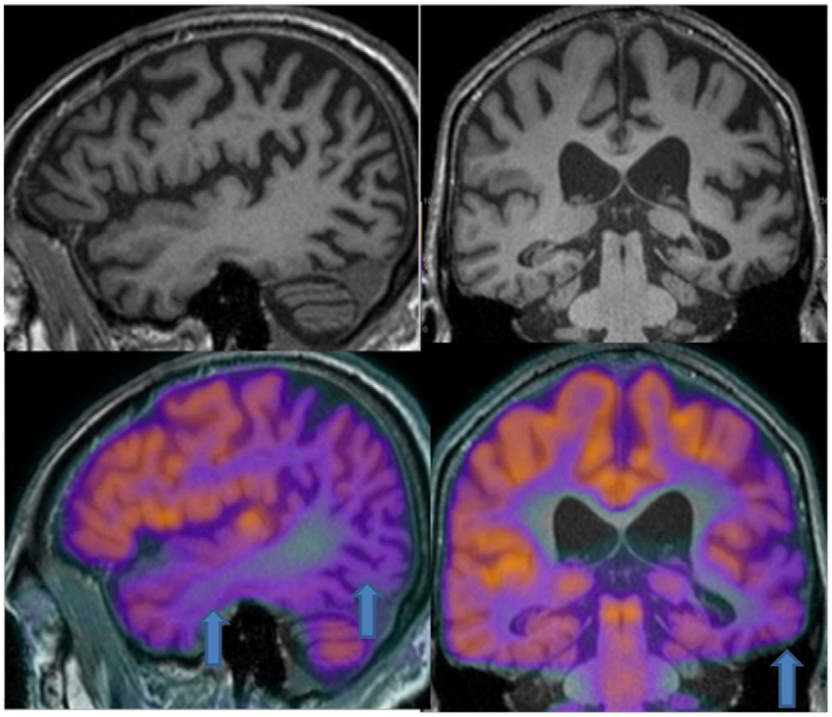

levels of Aβ, suggesting that PET amyloid imaging may have utility in detecting prodromal AD.[33] The new ^{18}F-labelled amyloid tracer under the commercial name of Florbetapir (AMY-ViD®; Eli Lilly and Company, Indianpolis, IN) has been recently introduced in many European countries including the UK. This compound showed a neuropathologically accurate and reliable estimation of the density of Aβ neuritic plaques in the brain, in both clinical and non-clinical studies. There is a growing interest among the research community to establish the clinical role of this new molecule in the management of patients with AD.

Structural MRI plays a central role in the evaluation of brain morphology in dementia, and volumetric assessment using dedicated software shows significant promise in the diagnosis of early-stage AD and for monitoring disease progression. Typical findings are medial temporal lobe atrophy in both mild cognitive impairment (MCI) and AD, especially in the entorhinal cortex, amygdala, hippocampus and parahippocampal gyrus.

A comparison between the metabolism and morphology of this complex region has only recently become possible with the development of simultaneous PET-MRI systems.[34] A preliminary experience in 2010 reported that the hippocampal glucose metabolism in patients with AD had a significantly decreased glucose metabolic function compared with normal controls.[35] Furthermore, combining MRI, ^{18}F-FDG-PET and CSF biomarkers yielded the highest accuracy for predicting conversion to AD in subjects with MCI.[36]

Clinical availability of the latest MRI sequences, such as arterial spin labelling (ASL) and diffusion tensor imaging (DTI) may provide additional information complementary to anatomical MRI and metabolic ^{18}F-FDG-PET.

ASL is a non-contrast MRI technique that uses magnetically labelled water protons as an endogenous tracer to provide information about blood flow. Important advantages of this technique are its non-invasiveness and relatively short acquisition time (at current clinical magnetic field strengths of 3.0 T), which enable routine application in the work-up of dementia.[37,38] A recent study reported matching patterns of reduced cerebral blood flow and ^{18}F-FDG-PET hypometabolism in patients with AD.[39]

DTI is a technique that allows the evaluation of brain axonal tract morphology. Software algorithms estimate the preferential direction of diffusion of water molecules from a series of images acquired with diffusion gradients applied at different spatial orientations. The preferential direction of diffusion reflects the orientation of axons and allows white matter neuronal pathways to be followed, and thus the global connectivity of the brain to be investigated. In AD, the use of DTI facilitates visualization of early white matter changes, which disrupt neuronal connectivity, a finding that confirms that disease effects are not simply confined to the cortex.[40]

The potential power of PET-MRI for AD arises from a combination of high-resolution anatomical, perfusion, tractography MRI information with ^{18}F-FDG- or ^{11}C-PiB-PET during a single simultaneous examination, creating opportunities for improving the understanding of pathogenesis and mechanism of AD and enabling early diagnosis and supporting drug development.

Epilepsy

The evaluation of areas of reduced metabolism coupled with detailed anatomical information is of interest not only in degenerative disease but also for the evaluation of the epileptogenic focus in drug-resistant epilepsy. A match between areas of hypometabolism and the epileptogenic focus has been demonstrated on interictal PET. Moreover, our preliminary results show a possible mismatch between metabolism and perfusion. It is worth highlighting that, in this disease, there may be discrepancies in either metabolism and/or tissue microstructure and/or vascularity, making the possible use of a combined simultaneous PET-MRI technique important for diagnosis and in treatment planning.

Intracranial neoplasms

In the UK, the incidence of new brain tumours is estimated as 15/100 000 people per year.[41]

MR is the established gold standard for the evaluation of brain tumours. Conventional MR sequences (T_1/T_2/fluid-attenuated inversion–recovery) provide high-resolution anatomical detail and are supplemented by gadolinium contrast-enhanced MRI for evaluation of vascular supply and blood–brain barrier (BBB) integrity.[42,43]

Nonetheless, conventional MRI techniques (including gadolinium enhancement) are not sufficiently tissue specific and have some significant clinical limitations. For example, gadolinium enhancement is a marker of BBB disruption and does not demonstrate tumour activity directly, and it has been reported that roughly 10% of glioblastomas and 30% of anaplastic astrocytomas do not show gadolinium enhancement.[44] Furthermore, gadolinium enhancement is not always specific for tumour grade, as low-grade gliomas occasionally enhance.[45] In recent years, there have been numerous investigations on the ability of functional and molecular imaging techniques, such as diffusion, perfusion and proton MR spectroscopy to assess tumour characteristics and treatment effect.[46,47]

Nuclear medicine, although generally considered the reference technique to assess metabolism, has been limited for many years by the lack of adequate tracers. ^{18}F-FDG as a glucose analogue represents the main substrate for the normal brain. As a consequence, there is diffuse uptake in the brain parenchyma, which impairs visualization of tumour foci. PET neuroimaging has therefore focused on the development of alternative tracers to ^{18}F-FDG. Available tracers evaluate amino acid metabolism, hypoxia and membrane turnover. Labelled amino acids and their analogues [L-[methyl-^{11}C]-methionine (^{11}C-Met), ^{11}C-tyrosine, ^{18}F-fluorotyrosine, ^{18}F-deoxyphenylalanine and ^{2}O-^{18}F-fluoroethyltyrosine] are particularly attractive because of their high uptake in tumour tissue and low uptake in normal brain. ^{18}F-fluoromisonidazole (^{18}F-FMISO) is a marker of blood flow and hypoxia.[48] Whilst ^{18}F-FMISO-PET demonstrates a correlation with perfusion at 0–5 min after injection, late persistent uptake remains independent of perfusion and BBB disruption and is correlated with hypoxia.[49,50] ^{18}F-choline is a biomarker of cell membrane turnover and increased uptake on PET reflects tumour aggressiveness and can be used to monitor tissue proliferation on follow-up (Figure 2).[51]

Simultaneous PET-MRI offers the potential to develop new applications based on multimodal multiparametric tumour assessment. For example, a recent article demonstrated the feasibility of simultaneous acquisition of PET-MRI for tumour grading and examining the spatial distribution of metabolic changes within a glioma.[52] All patients underwent simultaneous ^{11}C-MET multiparametric PET-MRI, for identification of the most aggressive part of the tumour to facilitate targeted surgical sampling. The authors concluded that metabolic mapping before histological sampling is feasible using simultaneous PET-MRI. An important observation made by the authors was that parameters from different modalities that are thought to reflect the same pathological processes do not necessarily spatially correlate. For instance, a high level of ^{11}C-MET uptake on PET, indicative of proliferating tumour cell populations, was not always colocalized to areas of cell membrane proliferation (choline/*N*-acetylaspartate) seen with MR spectroscopy; the observations suggest that combining PET and MRI methods could provide additional information about cellular proliferation, improve selection of biopsy sites and potentially separate tumour tissue better from scarring, inflammation and necrosis.

Figure 2. Images of an 11-year-old female with pathologically proven low-grade glioma (arrows). Axial image: (a) diffusion weighted image, (b) apparent diffusion coefficient (ADC) map and (c)^{18}F-choline-PET/T_1 MR fused. Moderate ^{18}F-choline uptake and mildly reduced ADC is present within the tumour.

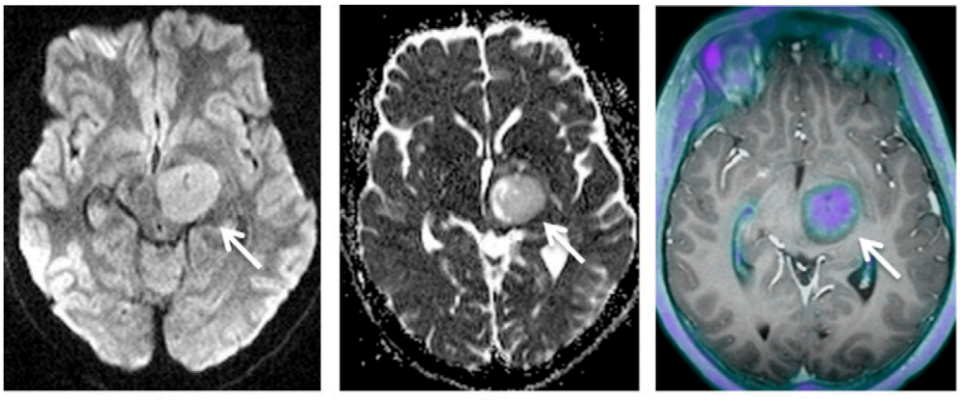

A further attractive application of PET-MRI is the pre- and post-operative evaluation of meningiomas. This tumour, although considered benign, often causes compression of important structures and, in a few cases, may show an aggressive behaviour (Figure 3).[53] Meningiomas located at the skull base are particularly difficult to treat because of their proximity to vital structures such as blood vessels, cranial nerves and the brainstem, and, in such cases, a multimodal therapeutic approach is frequently necessary.

In general, surgical resection is the treatment of choice for meningiomas; nevertheless, in the adjuvant setting, radiation therapy is also highly effective. Morphological imaging methods, such as CT and MRI, are commonly used for target volume definition in radiation therapy. However, whilst providing anatomical detail, they demonstrate limitations for tissue characterization, *i.e.* distinguishing between meningioma and other tissues, such as post-operative scars, skull base and other normal intracranial structures.[54,55] Hence, there is a need for additional methods to characterize tissue and more accurately determine the extension of meningioma into the neighbouring anatomical structures.

PET imaging offers a solution through high levels of expression of the somatostatin receptor subtype 2 in meningiomas, which can be targeted by somatostatin receptor ligands to provide an excellent tumour-to-background signal ratio.[56–59]

A PET-MRI solution combining gadolinium enhancement and somatostatin tracer uptake could have the potential to further improve pre-operative planning and to better monitor and localize recurrence following therapy.

BODY ONCOLOGICAL APPLICATIONS OF POSITRON EMISSION TOMOGRAPHY-MRI

PET-CT is widely used for cancer staging. Whilst the CT component aids the localization of the PET signal to the correct anatomical site, the non-contrast-enhanced CT provides little tissue characterization beyond the assessment of density. More recently, multiparametric MRI has emerged as the method of choice for tissue characterization and is rapidly establishing clinical utility, for example, in the localization and surveillance of prostate cancers.[60,61] Nonetheless, it remains more difficult to assess metabolic activity with MRI, and MRI signals themselves are not as specific as PET tracers. Simultaneous PET-MRI offers the ability to combine the power of MRI tissue characterization with targeted molecular PET imaging.

A simultaneous PET-MRI approach offers significant advantages for body oncological imaging. Techniques for registering separately acquired MRI and PET data have been evaluated[1–4,6] and remain operator dependent with inconsistent and poor results, particularly for deformable regions (*e.g.* the breast) or physiologically mobile structures (*e.g.* the intestinal tract and bladder). Moreover, there is often a significant physiological variation in functionality with time when acquiring temporally separated PET and MRI studies fundamentally limiting correlation of signals. The concurrent acquisition of multiparametric MRI and PET has the potential to reduce both spatial and temporal correlation errors.

The first simultaneous clinical whole-body PET-MRI scanner became commercially available in 2011. Early adopters of the hardware have been rapidly developing and evaluating a range of strategies for tumour assessment.

Initial reports comparing PET-CT and PET-MRI (with MRI performed for anatomical localization/attenuation correction) of mixed cancers are available. These early studies confirm that whole-body simultaneous PET-MRI is feasible within a relatively short acquisition time (20 min) and furthermore that neither the PET nor the MR image quality is significantly compromised by simultaneous acquisition. Importantly, the clinical performance of PET-MRI for detection of malignant lesions is reported as comparable to that of PET-CT.[5,62–65] The studies suggest that replacing the CT component of the PET-CT examination with MRI is possible. This in itself could provide patient benefit by reducing overall diagnostic radiation, of particular importance

Figure 3. Images of a 47-year-old male with a skull base meningioma following surgery, being considered as a candidate for radiotherapy. Positron emission tomography (PET)-CT images (a) demonstrate a ^{68}Ga-DOTATATE (derivative of octreotide)-avid lesion in the left middle cranial fossa. T_1 post-contrast MR images (b) show anatomical detail of the tumour location. Combined PET-MRI (c) allows visualization of the full extent of this disease.

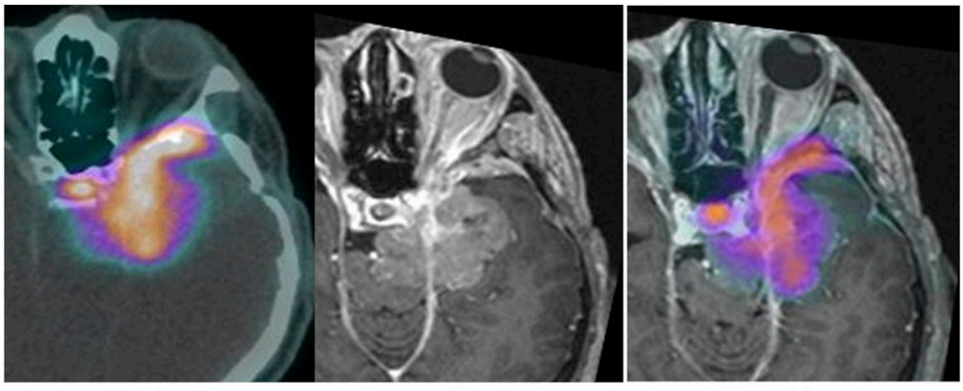

(a) (b) (c)

for paediatric and adolescent patients or those requiring multiple sequential studies. Indeed, a report of 15 children with multifocal malignant diseases concluded that the effective dose of simultaneous PET-MRI scan was only 20% that of the equivalent PET-CT examination.[66]

Whilst reduction in radiation dose is important, compared with CT, detecting and characterizing lung lesions on MRI remains challenging and requires the use of respiratory gating, which may be imperfect, or rapid breath-hold acquisition, which limits spatial resolution.[67] Additionally, although the 3-T MRI included within the simultaneous PET-MRI machine can provide additional signal, susceptibility artefacts at air–tissue interfaces are also increased, making imaging the lungs more challenging at 3 T than at 1.5 T. Nevertheless, perfect anatomical MRI of the lungs may not be necessary. A combined PET-MRI examination could benefit from the sensitivity of PET tracer for detection/characterization of clinically significant lung nodules and may compensate for the limitations of MRI. Indeed, preliminary data on pulmonary lesion assessment performed in 10 patients who underwent PET-CT and, immediately afterwards, PET-MRI with anatomical whole-body MRI support this view. Within this study, PET-MRI provided diagnostic image quality in all patients, with good tumour delineation, allowing similar lesion characterization and tumour staging to PET-CT (Figure 4).[68]

Multiparametric MRI techniques for evaluation of suspect lesions are also being explored (Figure 5).[69] Such studies will help to refine simultaneous PET-MRI protocols; for example, as the ^{18}F-FDG signal correlates with the diffusion-weighted MR signal, the additional time spent acquiring MRI "functional" data could be regarded as superfluous for diagnosis.[70] These PET-MRI studies also provide an opportunity for correlative cross-modality biomarker research and a broadened approach to understanding mechanisms of disease; for example, applications include colorectal cancer, gynaecological disease or soft-tissue tumours (Figures 6–9). Ultimately, as functional MRI and PET signals are correlated, *e.g.* ^{18}F-FDG-PET and MRI apparent diffusion coefficient, it may become possible to substitute the PET signal with the functional MRI signal, thereby allowing the use of an alternative radionuclide tracer to evaluate a second biological tumour characteristic (*e.g.* hypoxia or angiogenesis).

Lymphoma

There has been much work on the role of PET-CT and, more recently, the application of whole-body MRI for evaluation of lymphoma.[71] Increased glucose metabolism is common to most lymphoma subtypes, and PET with ^{18}F-FDG has become an established modality for lymphoma staging and follow-up.[72] A recent study demonstrated the feasibility of ^{18}F-FDG-PET-MRI for lymphoma treatment response evaluation and reported good image quality of the PET-MRI examination and an excellent interobserver agreement for Ann Arbor stage;[63] experience at our institution supports this finding (Figure 10).

Prostate cancer

There has been a significant drive in the application of multiparametric MRI for localization of prostate cancer prior to biopsy and treatment.[73,74] However, it is recognized that assessment of the post-treatment prostate and local nodal disease remains challenging even with multiparametric MRI. ^{18}F-choline-PET has shown promise for the clinical staging of metastatic prostate cancer, and results also show that it has a potential role in assessing the post-therapy gland.[75] A number of centres are exploring combined PET-MRI acquisitions using whole-body ^{18}F-choline-PET paired with anatomical whole-body MRI and multiparametric prostate MRI in the hope that a single test will be able to identify and stage local tumour, together with metastatic nodal and bone disease (Figure 11). Early reports suggest a high concordance between ^{18}F-choline-PET and diffusion-weighted MRI signals; however, PET-positive lesions have also been demonstrated within the prostate, where diffusion-weighted imaging has not suggested tumour.[76]

Head and neck squamous cell carcinoma

Preliminary experience of PET-MRI in 20 patients with histologically proven head and neck squamous cell carcinoma has been reported in a study comparing the performance of PET-MRI *vs* stand-alone PET.[77] The number of lymph nodes with increased ^{18}F-FDG uptake detected using the PET data set from the simultaneous PET-MRI system was significantly higher than the number from the stand-alone PET scanner.

Neuroendocrine tumours

Evaluating patients with neuroendocrine tumours is a further potential application of simultaneous PET-MRI. PET-CT with somatostatin analogues such as [^{68}Ga]-DOTATATE (derivative of octreotide) is routinely used to stage and evaluate the therapy response of neuroendocrine tumours,[78] although the current weakness of PET-CT remains the difficulty in detecting neuroendocrine liver metastases where the physiological somatostatin

Figure 4. Images of a 68-year-old male with a small (approximately 1 cm diameter) lung nodule. Concordant nodule detection on (a) positron emission tomography (PET)-MRI, (b) PET-CT and (c) contrast-enhanced CT.

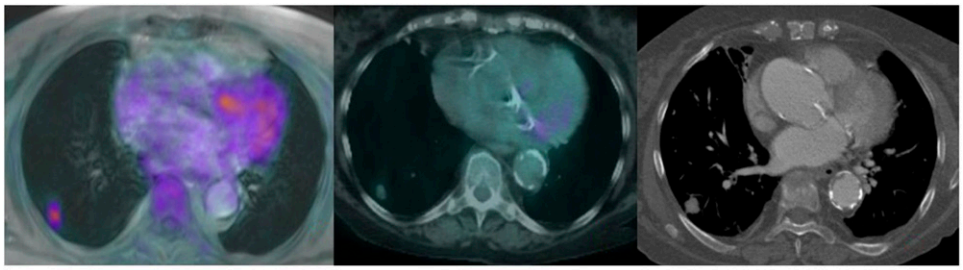

Figure 5. Images of a 58-year-old male with a large colorectal cancer imaged using simultaneous multiparametric MRI and positron emission tomography (PET) for multimodal tumour characterization. Arrows indicate tumour: (a) axial T_2 weighted images, (b) apparent diffusion coefficient map, (c) ^{18}F-fludeoxyglucose-PET-MRI fused images with avid uptake of tracer. (d, e) Early and delayed contrast enhancement extracted from a dynamic contrast-enhanced series. (f) Maximum intensity projection image demonstrating collateral vessels feeding the neoplasm.

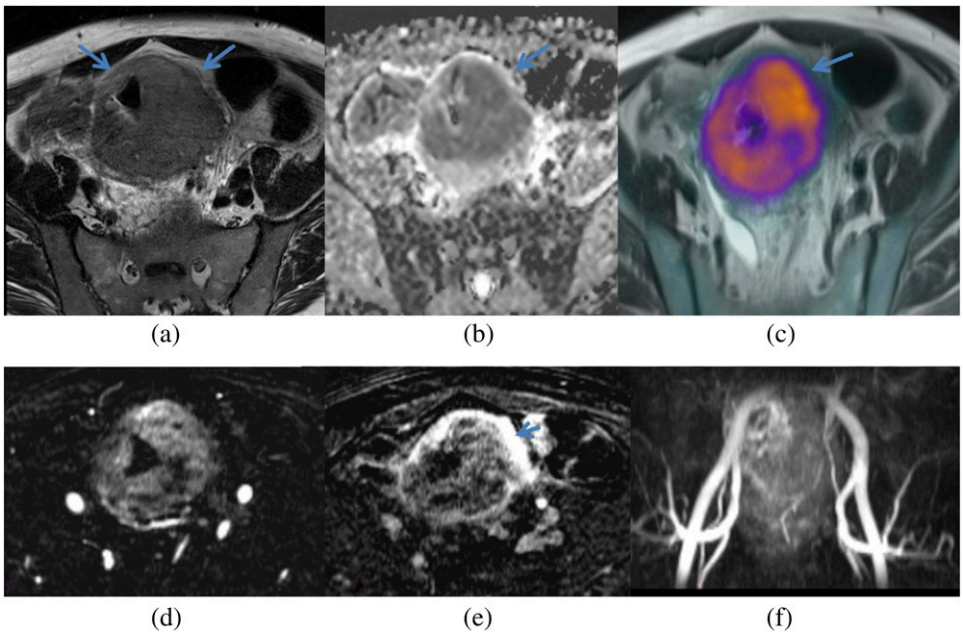

tracer uptake can mask small lesions. Our initial experience suggests that combining PET with a localized dynamic contrast-enhanced MRI of the liver and whole-body anatomical MRI could improve disease assessment (Figure 12).

Figure 6. Multiparametric MRI is acquired simultaneously with ^{18}F-fludeoxyglucose (^{18}F-FDG) positron emission tomography (PET). Anatomical out-of-phase MR images (d) show poor lesion contrast (arrow); however, the lesion is well depicted on the attenuation-corrected PET image (b) and corresponding fused PET-MRI image (a). ^{18}F-FDG uptake inversely correlates with restriction of diffusion depicted on the apparent diffusion coefficient map (c) (arrow).

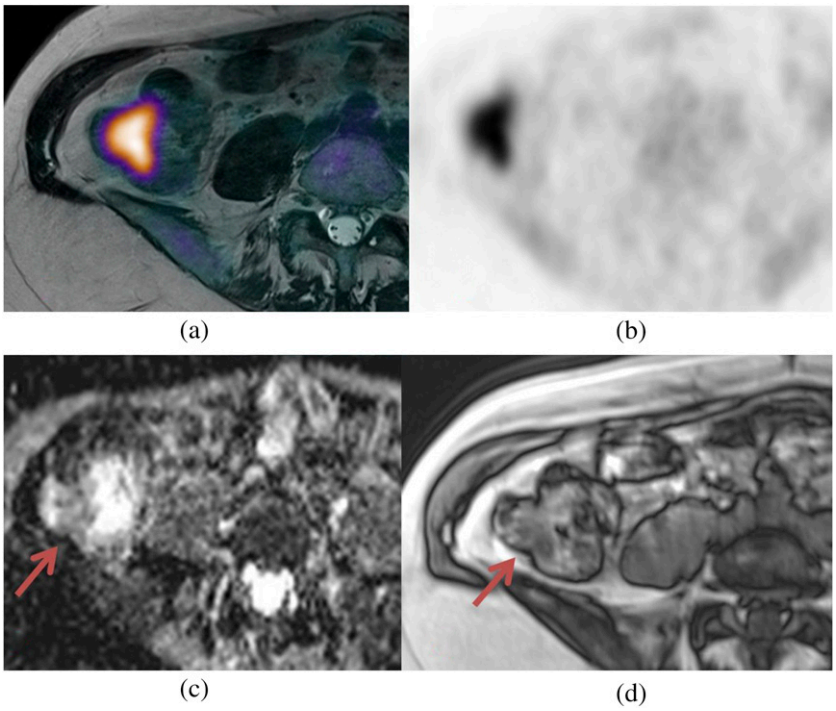

Figure 7. Multiparametric evaluation of a cervical carcinoma (arrows). (a) Axial and (b) sagittal: fused positron emission tomography-MRI (anatomical T_2 weighted image) with increased ^{18}F-fludeoxyglucose uptake within the tumour. (c) Apparent diffusion coefficient map with restricted diffusion.

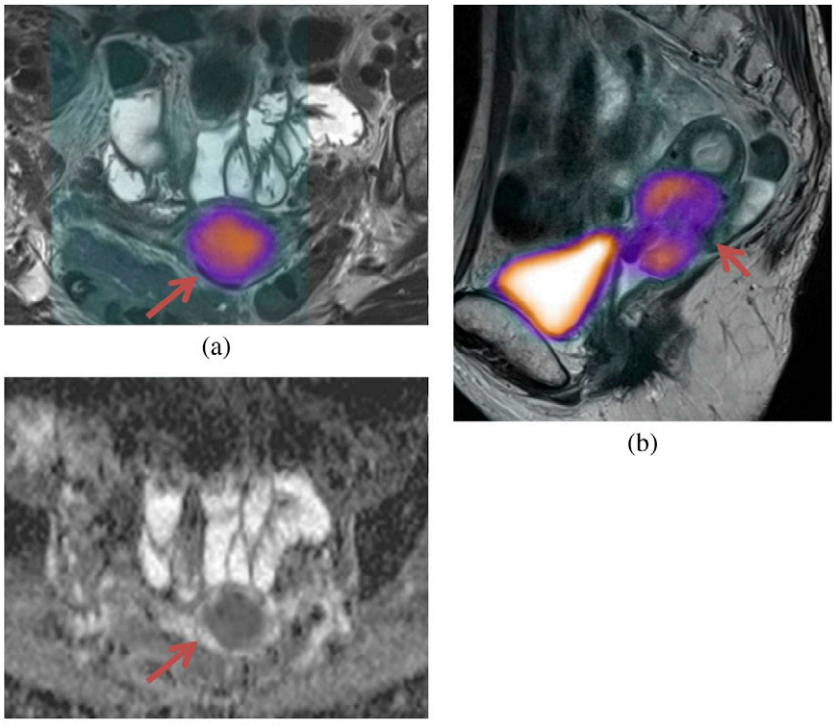

Gastrointestinal tumours

PET-CT is used for the initial metastatic staging and assessment of suspected recurrence of colorectal cancer.[79] Local staging, particularly that for rectal cancer, is best performed with dedicated MRI protocols.[80] A weakness of PET-CT remains the visualization of small liver metastases.[81] Indeed, based on reconstructive data sets, Yong et al[82] suggest that PET-MRI is likely to have greater sensitivity than PET-CT (98.3% *vs* 84.2%). The challenge remains to determine whether the MRI component of the PET-MRI study can be adapted such that a single PET-MRI study can provide local staging and improve metastatic disease localization.

Figure 8. Axial positron emission tomography-MRI (anatomical T_2 weighted image) of an oesophageal tumour with perivisceral infiltration (arrowheads).

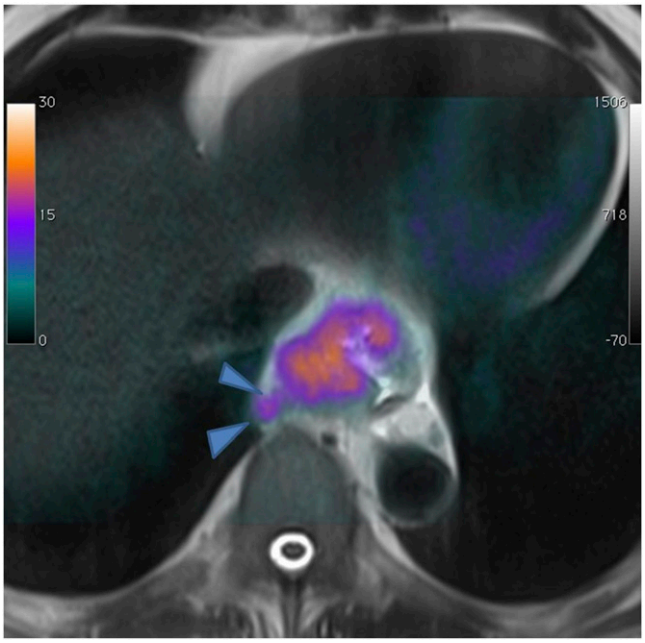

Application of PET-MRI for assessment of oesophageal tumours is likely to be more difficult than for colorectal cancer, as increased artefacts resulting from respiratory motion, cardiac motion and susceptibility at air–tissue interfaces need to be mitigated.

Gynaecological tumours

At present, the diagnosis of ovarian cancer is based on clinical examination and serum biomarkers combined with localized imaging with ultrasound, CT or MRI.[83] PET-CT using FDG as a non-specific tracer and with the limited resolution of PET is not the modality of choice for local staging of primary disease.[84] For metastatic staging, reports demonstrate that PET-CT is consistent with surgical staging in 69–78% of patients.[85,86] MRI with diffusion-weighted imaging has been reported to have a higher performance for the detection of peritoneal disease spread;[87] however, lymph node metastases remain difficult to characterize in normal sized nodes.[88] A complete technique that provides local staging of tumour with diagnostic MRI combined with anatomical and diffusion-weighted PET-MRI for metastatic disease evaluation should be explored.

Figure 9. (a) Coronal short tau inversion–recovery MRI shows multiple areas of increased abnormal signal in the vertebra (thin arrows) and left iliac wing (thick arrows). (b) Active disease is differentiated from stable disease on the combined positron emission tomography-MRI as areas of increased ^{18}F-fludeoxyglucose uptake.

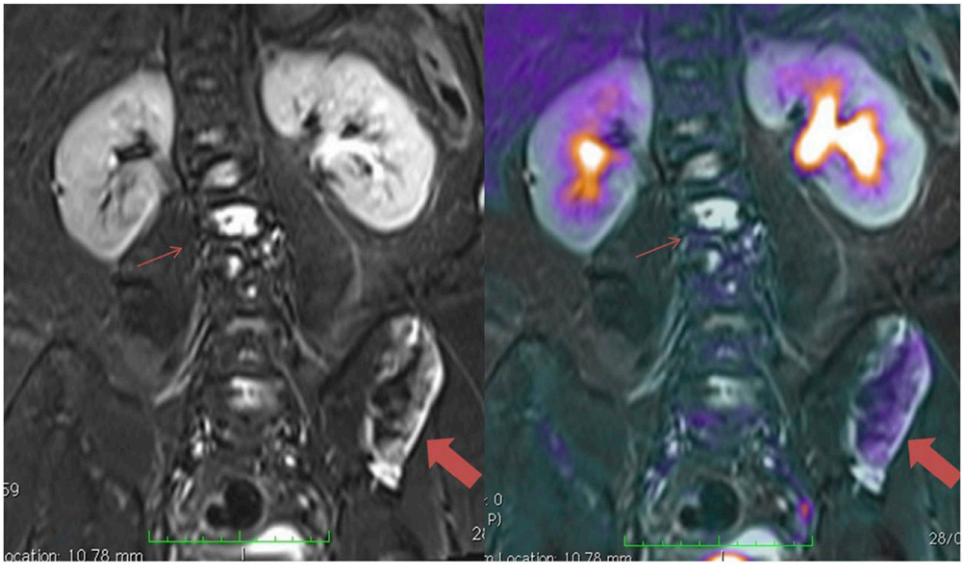

(a) (b)

Similarly, cervical and uterine cancers are likely to also require dedicated local MRI staging protocols to be combined with whole-body PET-MRI metastatic disease staging.

Musculoskeletal tumours

MRI and plain radiographs are the core imaging modalities used for the assessment of bone tumours.[89] It is difficult to visualize how PET-MRI could improve the local staging and assessment of this group of tumours. In keeping with other tumour types, the benefit of a PET-MRI examination is likely to be in the assessment of nodal stage. For patients with bone tumours, PET-CT has a reported sensitivity and specificity of 88% and 97%, respectively, for nodal staging, higher than conventional staging methods.[90] Other than exploiting the capability of PET, it is

Figure 10. ^{18}F-fludeoxyglucose positron emission tomography (PET) CT scan (thick multiplanar reformat) (a) shows multiple confluent nodes above and below the diaphragm. Multiple liver lesions are also seen. Cross-sectional PET-MRI (b) maximum intensity projection and (c) volume-rendered reconstruction show similar appearances.

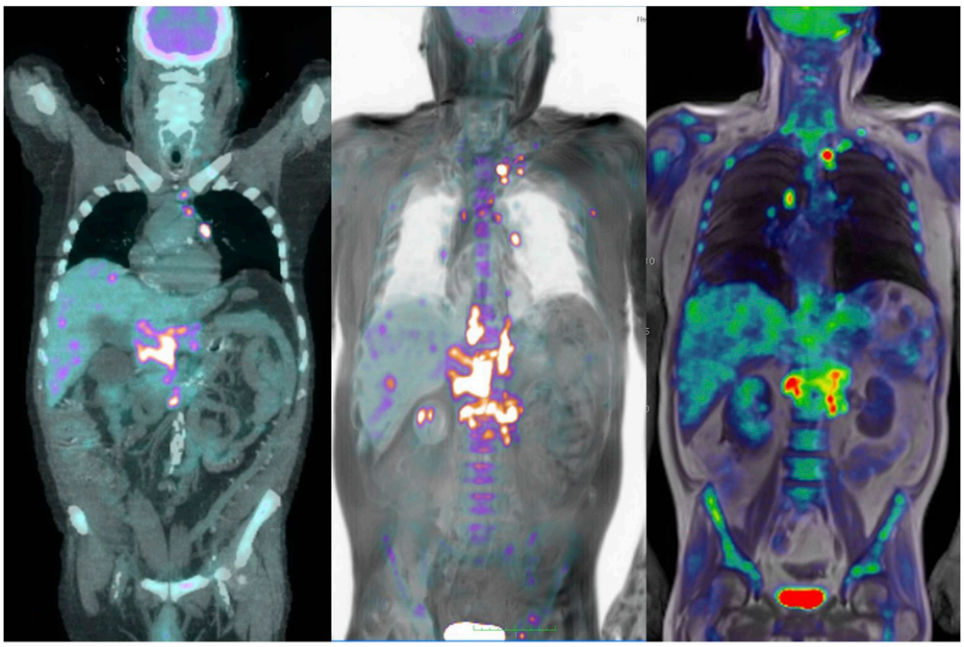

(a) (b) (c)

Figure 11. ^{18}F-choline positron emission tomography (PET) demonstrating a large choline-avid lesion suspicious for tumour (arrow). Superior anatomical detail is provided by the anatomical MRI (a) fused PET-MRI compared with CT (b) fused PET-CT.

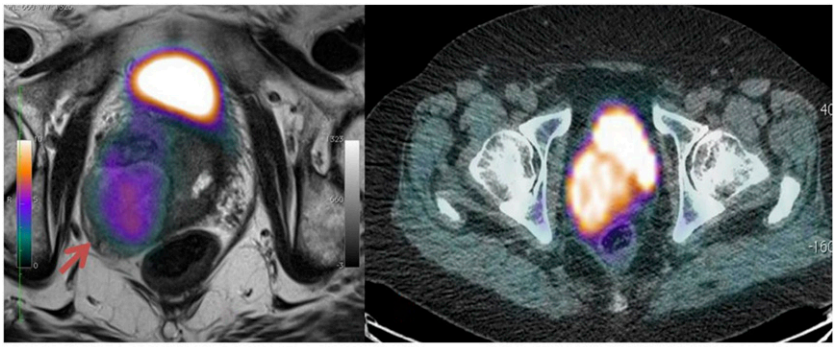

(a) (b)

uncertain whether a PET-MRI technique for initial staging will have additional benefit.

An area of development for PET-MRI within this group could be in response assessment. Both PET and MRI methods when performed separately have demonstrated encouraging results for restaging,[91,92] and the performance of a PET-MRI technique that exploits the merits of both remains an area of research.

CARDIOVASCULAR

PET-MRI for assessment of cardiovascular disease may truly exploit and require simultaneous acquisition of PET and MRI signals. PET is the gold standard for non-invasive assessment of myocardial viability.[93] For the first time, simultaneous PET-MRI can provide direct comparison of the diagnostic performance of each modality at identical resting and stress conditions. MRI provides high-resolution anatomical imaging that allows accurate evaluation of ventricular structure and function together with detection of myocardial infarction.[94] Furthermore, there is the potential for morphological information obtained by MRI to be combined with PET functional imaging, *e.g.* to help differentiate between epicardial stenosis and microvascular dysfunction or between a scar and dysfunctional but viable myocardium.[95]

PET-MRI provides an opportunity to follow molecular and cellular events after myocardial infarction. Delayed enhancement MRI after injection of gadolinium-diethylenetriaminepentaacetate can delineate the infarcted myocardium,[96] whereas the PET signal reflects at the same time the viable myocardium.[97] The combination of the two modalities was recently investigated and showed close agreement between contrast-enhanced MRI and PET in detecting transmural myocardial scars. There is little experience with combining MRI and PET for evaluation of subendocardial tissue for differentiating between scar and viability.

Studies focusing on tracers other than ^{18}F-FDG may exploit the capabilities of simultaneous cardiac PET-MRI, *e.g.* anatomical MRI combined with the imaging of angiogenesis[98,99] and sympathetic dysfunction associated with heart failure.[85]

MRI has previously been proposed for studying inflammation,[100] but there are limitations related to difficulty in characterizing acute, subacute and early chronic disease;[101]

Figure 12. ^{68}Ga-DOTATATE positron emission tomography-MRI (a) shows a focal avid liver lesion (arrows), difficult to see even with contrast-enhanced MRI (b).

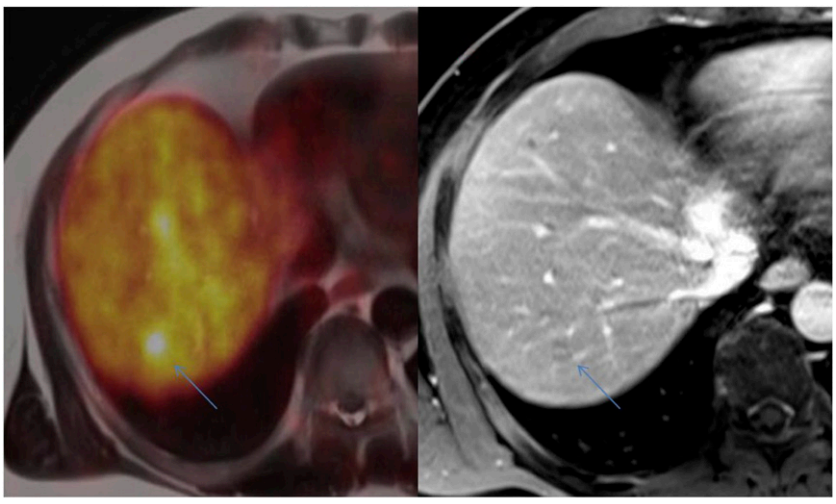

(a) (b)

a hybrid approach for both myocarditis and pericarditis may improve results. Cardiac sarcoidosis represents another inflammatory cardiomyopathy for which simultaneous PET-MRI could be useful. In cardiac sarcoidosis, the myocardium is replaced by fibrotic fibrogranulomatous tissue. As potential application, fibrotic changes could be evaluated by MRI (*e.g.* equilibrium MRI[102]) and simultaneous PET imaging could characterize patterns of glucose metabolism related to the different stages of disease.

INFLAMMATORY DISEASE

Advances in multidetector CT and MRI pulse sequences have improved anatomical detail and tissue characterization of inflammatory diseases.[103] Several efforts have been made to combine new MR contrast agents with PET imaging (*e.g.* atherosclerotic plaque has been imaged *in vivo* using FDG and an ultrasmall superparamagnetic iron oxide MR agent[104]). The arrival of PET-MRI is likely to further consolidate this approach.[105] Indeed, there is an interest in developing and assessing MRI contrast agents labelled with PET tracer, where MR contrast agents are used to provide high-resolution anatomical detail of the location of accumulated metabolic PET tracer activity within plaques.[106,107]

Another interesting prospective use of PET-MRI is in the assessment of inflammatory bowel disease. There is growing experience in the assessment of inflammatory bowel disease with MRI,[108] but sensitivity for early disease and the differentiation of fibrotic and inflammatory strictures remain problematic.[109] A simultaneous PET-MRI approach could be explored to determine if metabolic PET information can complement MRI and thereby guide therapy.

CONCLUSION

Currently, simultaneous PET-MRI has the potential to improve patient care by reducing radiation dose, reducing hospital visits and potentially providing new and more specific/sensitive markers for disease assessment. Early proof-of-concept studies are encouraging and show that the clinical performance of PET-MRI is on a par with PET-CT. The next step will be to generate initial clinical applications together with optimized protocols for subsequent validation and evaluation of clinical benefit. Much work remains to be done before the techniques can become part of a standard clinical diagnostic pathway.

FUNDING

This work was supported by the National Institute for Health Research University College London Hospitals Biomedical Research Centre.

ACKNOWLEDGMENTS

The authors would like to thank colleagues within the Institute of Nuclear Medicine for providing the figures in support of this article.

REFERENCES

1. Zaidi H, Montandon ML, Alavi A. The clinical role of fusion imaging using PET, CT, and MR imaging. *Magn Reson Imaging Clin N Am* 2010; **18**: 133–49. doi: 10.1016/j.mric.2009.09.010
2. Karlo CA, Steurer-Dober I, Leonardi M, Pfirrmann CW, Zanetti M, Hodler J. MR/CT image fusion of the spine after spondylodesis: a feasibility study. *Eur Spine J* 2010; **19**: 1771–5.
3. Pichler BJ, Judenhofer MS, Wehrl HF. PET/MRI hybrid imaging: devices and initial results. *Eur Radiol* 2008; **18**: 1077–86. doi: 10.1007/s00330-008-0857-5
4. Herzog H, Van Den Hoff J. Combined PET/MR systems: an overview and comparison of currently available options. *Q J Nucl Med Mol Imaging* 2012; **56**: 247–67.
5. Kalemis A, Delattre BM, Heinzer S. Sequential whole-body PET/MR scanner: concept, clinical use, and optimisation after two years in the clinic. The manufacturer's perspective. *MAGMA* 2013; **26**: 5–23. doi: 10.1007/s10334-012-0330-y
6. Peng MJ, Ju X, Khambay BS, Ayoub AF, Chen CT, Bai B. Clinical significance of creative 3D-image fusion across multimodalities [PET+CT+MR] based on characteristic coregistration. *Eur J Radiol* 2012; **81**: e406–13. doi: 10.1016/j.ejrad.2011.12.031
7. Delso G, Fürst S, Jakoby B, Ladebeck R, Ganter C, Nekolla SG, et al. Performance measurements of the Siemens mMR integrated whole-body PET/MR scanner. *J Nucl Med* 2011; **52**: 1914–22. doi: 10.2967/jnumed.111.092726
8. Catana C, Wu Y, Judenhofer MS, Qi J, Pichler BJ, Cherry SR. Simultaneous acquisition of multislice PET and MR images: initial results with a MR-compatible PET scanner. *J Nucl Med* 2006; **47**: 1968–76.
9. Heiss WD. The potential of PET/MR for brain imaging. *Eur J Nucl Med Mol Imaging* 2009; **36**(Suppl. 1): S105–12. doi: 10.1007/s00259-008-0962-3
10. Judenhofer MS, Catana C, Swann BK, Siegel SB, Jung WI, Nutt RE, et al. PET/MR images acquired with a compact MR-compatible PET detector in a 7-T magnet. *Radiology* 2007; **244**: 807–14. doi: 10.1148/radiol.2443061756
11. Schlemmer HP, Pichler BJ, Schmand M, Burbar Z, Michel C, Ladebeck R, et al. Simultaneous MR/PET imaging of the human brain: feasibility study. *Radiology* 2008; **248**: 1028–35. doi: 10.1148/radiol.2483071927
12. Dixon WT. Simple proton spectroscopic imaging. *Radiology* 1984; **153**: 189–94. doi: 10.1148/radiology.153.1.6089263
13. Yeung HN, Kormos DW. Separation of true fat and water images by correcting magnetic field inhomogeneity in situ. *Radiology* 1986; **159**: 783–6. doi: 10.1148/radiology.159.3.3704157
14. Berker Y, Franke J, Salomon A, Palmowski M, Donker HC, Temur Y, et al. MRI-based attenuation correction for hybrid PET/MRI systems: a 4-class tissue segmentation technique using a combined ultrashort-echo-time/Dixon MRI sequence. *J Nucl Med* 2012; **53**: 796–804.
15. Hofmann M, Bezrukov I, Mantlik F, Aschoff P, Steinke F, Beyer T, et al. MRI-based attenuation correction for whole-body PET/MRI: quantitative evaluation of segmentation- and atlas-based methods. *J Nucl Med* 2011; **52**: 1392–9. doi: 10.2967/jnumed.110.078949
16. Johansson A, Karlsson M, Nyholm T. CT substitute derived from MRI sequences with ultrashort echo time. *Med Phys* 2011; **38**: 2708–14.
17. Martinez-Möller A, Nekolla SG. Attenuation correction for PET/MR: problems,

novel approaches and practical solutions. *Z Med Phys* 2012; **22**: 299–310. doi: 10.1016/j.zemedi.2012.08.003

18. Pauly O, Glocker B, Criminisi A, Mateus D, Möller AM, Nekolla S, et al. Fast multiple organ detection and localization in whole-body MR dixon sequences. *Med Image Comput Comput Assist Interv* 2011; **14**(Pt 3): 239–47.
19. Schmidt GP, Reiser MF, Baur-Melnyk A. Whole-body MRI for the staging and follow-up of patients with metastasis. *Eur J Radiol* 2009; **70**: 393–400. doi: 10.1016/j.ejrad.2009.03.045
20. Grant K, Lindenberg ML, Shebel H, Pang Y, Agarwal HK, Bernardo M, et al. Functional and molecular imaging of localized and recurrent prostate cancer. *Eur J Nucl Med Mol Imaging* 2013; **40**(Suppl. 1): S48–59. doi: 10.1007/s00259-013-2419-6
21. Wetter A, Lipponer C, Nensa F, Beiderwellen K, Olbricht T, Rubben H, et al. Simultaneous 18F choline positron emission tomography/magnetic resonance imaging of the prostate: initial results. *Invest Radiol* 2013; **48**: 256–62. doi: 10.1097/RLI.0b013e318282c654
22. Schwenzer NF, Stegger L, Bisdas S, Schraml C, Kolb A, Boss A, et al. Simultaneous PET/MR imaging in a human brain PET/MR system in 50 patients–current state of image quality. *Eur J Radiol* 2012; **81**: 3472–8. doi: 10.1016/j.ejrad.2011.12.027
23. Alzheimer A, Stelzmann RA, Schnitzlein HN, Murtagh FR. An English translation of Alzheimer's 1907 paper, "Uber eine eigenartige Erkankung der Hirnrinde". *Clin Anat* 1995; **8**: 429–31. doi: 10.1002/ca.980080612
24. Heron M, Hoyert DL, Murphy SL, Xu J, Kochanek KD, Tejada-Vera B. Deaths: final data for 2006. *Natl Vital Stat Rep* 2009; **57**: 1–134.
25. Jack CR Jr. Alzheimer disease: new concepts on its neurobiology and the clinical role imaging will play. *Radiology* 2012; **263**: 344–61. doi: 10.1148/radiol.12110433
26. Ewers M, Insel PS, Stern Y, Weiner MW; Alzheimer's Disease Neuroimaging Initiative. Cognitive reserve associated with FDG-PET in preclinical Alzheimer disease. *Neurology* 2013; **80**: 1194–201. doi: 10.1212/WNL.0b013e31828970c2
27. Foster NL, Chase TN, Fedio P, Patronas NJ, Brooks RA, Di Chiro G. Alzheimer's disease: focal cortical changes shown by positron emission tomography. *Neurology* 1983; **33**: 961–5.
28. Protas HD, Chen K, Langbaum JB, Fleisher AS, Alexander GE, Lee W, et al. Posterior cingulate glucose metabolism, hippocampal glucose metabolism, and hippocampal volume in cognitively normal, late-middle-aged persons at 3 levels of genetic risk for Alzheimer disease. *JAMA Neurol* 2013; **70**: 320–5. doi: 10.1001/2013.jamaneurol.286
29. Choo IH, Ni R, Scholl M, Wall A, Almkvist O, Nordberg A. Combination of (18)F-FDG PET and cerebrospinal fluid biomarkers as a better predictor of the progression to Alzheimer's disease in mild cognitive impairment patients. *J Alzheimers Dis* 2013; **33**: 929–39. doi: 10.3233/JAD-2012-121489
30. Mathis CA, Wang Y, Holt DP, Huang GF, Debnath ML, Klunk WE. Synthesis and evaluation of 11C-labeled 6-substituted 2-arylbenzothiazoles as amyloid imaging agents. *J Med Chem* 2003; **46**: 2740–54. doi: 10.1021/jm030026b
31. Rowe CC, Ackerman U, Browne W, Mulligan R, Pike KL, O'Keefe G, et al. Imaging of amyloid beta in Alzheimer's disease with 18F-BAY94-9172, a novel PET tracer: proof of mechanism. *Lancet Neurol* 2008; **7**: 129–35. doi: 10.1016/S1474-4422(08)70001-2
32. Serdons K, Verduyckt T, Vanderghinste D, Cleynhens J, Borghgraef P, Vermaelen P, et al. Synthesis of 18F-labelled 2-(4′-fluorophenyl)-1,3-benzothiazole and evaluation as amyloid imaging agent in comparison with [11C]PIB. *Bioorg Med Chem Lett* 2009; **19**: 602–5. doi: 10.1016/j.bmcl.2008.12.069
33. Stark SL, Roe CM, Grant EA, Hollingsworth H, Benzinger TL, Fagan AM, et al. Preclinical Alzheimer disease and risk of falls. *Neurology* 2013; **81**: 437–43. doi: 10.1212/WNL.0b013e31829d8599
34. Cho ZH, Son YD, Kim HK, Kim KN, Oh SH, Han JY, et al. A fusion PET-MRI system with a high-resolution research tomograph-PET and ultra-high field 7.0 T-MRI for the molecular-genetic imaging of the brain. *Proteomics* 2008; **8**: 1302–23. doi: 10.1002/pmic.200700744
35. Cho ZH, Son YD, Kim HK, Kim ST, Lee SY, Chi JG, et al. Substructural hippocampal glucose metabolism observed on PET/MRI. *J Nucl Med* 2010; **51**: 1545–8. doi: 10.2967/jnumed.110.076182
36. Shaffer JL, Petrella JR, Sheldon FC, Choudhury KR, Calhoun VD, Coleman RE, et al. Predicting cognitive decline in subjects at risk for Alzheimer disease by using combined cerebrospinal fluid, MR imaging, and PET biomarkers. *Radiology* 2013; **266**: 583–91. doi: 10.1148/radiol.12120010
37. Paiva FF, Tannus A, Silva AC. Measurement of cerebral perfusion territories using arterial spin labelling. *NMR Biomed* 2007; **20**: 633–42. doi: 10.1002/nbm.1177
38. Petersen ET, Zimine I, Ho YC, Golay X. Non-invasive measurement of perfusion: a critical review of arterial spin labelling techniques. *Br J Radiol* 2006; **79**: 688–701. doi: 10.1259/bjr/67705974
39. Binnewijzend MA, Kuijer JP, Benedictus MR, van der Flier WM, Wink AM, Wattjes MP, et al. Cerebral blood flow measured with 3D pseudocontinuous arterial spin-labeling MR imaging in Alzheimer disease and mild cognitive impairment: a marker for disease severity. *Radiology* 2013; **267**: 221–30. doi: 10.1148/radiol.12120928
40. Shu N, Liang Y, Li H, Zhang J, Li X, Wang L, et al. Disrupted topological organization in white matter structural networks in amnestic mild cognitive impairment: relationship to subtype. *Radiology* 2012; **265**: 518–27. doi: 10.1148/radiol.12112361
41. Cancer Research UK. Brain, other CNS and intracranial tumours incidence statistics [updated 28 March 2013; cited 17 July 2013]. Available from: http://www.cancerresearchuk.org/cancer-info/cancerstats/types/brain/incidence/
42. Price SJ, Gillard JH. Imaging biomarkers of brain tumour margin and tumour invasion. *Br J Radiol* 2011; **84**: S159–67. doi: 10.1259/bjr/26838774
43. Yuh WT, Christoforidis GA, Koch RM, Sammet S, Schmalbrock P, Yang M, et al. Clinical magnetic resonance imaging of brain tumors at ultrahigh field: a state-of-the-art review. *Top Magn Reson Imaging* 2006; **17**: 53–61. doi: 10.1097/RMR.0b013e3180300404
44. Scott JN, Brasher PM, Sevick RJ, Rewcastle NB, Forsyth PA. How often are non-enhancing supratentorial gliomas malignant? A population study. *Neurology* 2002; **59**: 947–9.
45. Knopp EA, Cha S, Johnson G, Mazumdar A, Golfinos JG, Zagzag D, et al. Glial neoplasms: dynamic contrast-enhanced T2*-weighted MR imaging. *Radiology* 1999; **211**: 791–8.
46. Al-Okaili RN, Krejza J, Wang S, Woo JH, Melhem ER. Advanced MR imaging techniques in the diagnosis of intraaxial brain tumors in adults. *Radiographics* 2006; **26** (Suppl. 1): S173–89. doi: 10.1148/rg.26si065513
47. Law M, Yang S, Wang H, Babb JS, Johnson G, Cha S, et al. Glioma grading: sensitivity, specificity, and predictive values of perfusion MR imaging and proton MR spectroscopic imaging compared with conventional MR imaging. *AJNR Am J Neuroradiol* 2003; **24**: 1989–98.
48. Gulyas B, Halldin C. New PET radiopharmaceuticals beyond FDG for brain

tumor imaging. *Q J Nucl Med Mol Imaging* 2012; **56**: 173–90.
49. Galban CJ, Chenevert TL, Meyer CR, Tsien C, Lawrence TS, Hamstra DA, et al. The parametric response map is an imaging biomarker for early cancer treatment outcome. *Nat Med* 2009; **15**: 572–6. doi: 10.1038/nm.1919
50. Hirata K, Terasaka S, Shiga T, Hattori N, Magota K, Kobayashi H, et al. (1)(8)F-Fluoromisonidazole positron emission tomography may differentiate glioblastoma multiforme from less malignant gliomas. *Eur J Nucl Med Mol Imaging* 2012; **39**: 760–70.
51. Tan H, Chen L, Guan Y, Lin X. Comparison of MRI, F-18 FDG, and 11C-choline PET/CT for their potentials in differentiating brain tumor recurrence from brain tumor necrosis following radiotherapy. *Clin Nucl Med* 2011; **36**: 978–81. doi: 10.1097/RLU.0b013e31822f68a6
52. Bisdas S, Ritz R, Bender B, Braun C, Pfannenberg C, Reimold M, et al. Metabolic mapping of gliomas using hybrid MR-PET imaging: feasibility of the method and spatial distribution of metabolic changes. *Invest Radiol* 2013; **48**: 295–301. doi: 10.1097/RLI.0b013e31827188d6
53. Black PM. *Cancer of the nervous system*. Oxford, UK: Blackwell Science; 1997.
54. McCutcheon IE. Stereotactic radiosurgery for malignant extracerebral intracranial tumors: patient selection, efficacy, and technical nuances. *Acta Neurochir Suppl* 2013; **116**: 71–83. doi: 10.1007/978-3-7091-1376-9_12
55. Mohan S, Hoeffner E, Bigelow DC, Loevner LA. Applications of magnetic resonance imaging in adult temporal bone disorders. *Magn Reson Imaging Clin N Am* 2012; **20**: 545–72. doi: 10.1016/j.mric.2012.06.001
56. Afshar-Oromieh A, Giesel FL, Linhart HG, Haberkorn U, Haufe S, Combs SE, et al. Detection of cranial meningiomas: comparison of (6)(8)Ga-DOTATOC PET/CT and contrast-enhanced MRI. *Eur J Nucl Med Mol Imaging*. 2012; **39**: 1409–15. doi: 10.1007/s00259-012-2155-3
57. Henze M, Dimitrakopoulou-Strauss A, Milker-Zabel S, Schuhmacher J, Strauss LG, Doll J, et al. Characterization of 68Ga-DOTA-D-Phe1-Tyr3-octreotide kinetics in patients with meningiomas. *J Nucl Med*. 2005; **46**: 763–9.
58. Henze M, Schuhmacher J, Hipp P, Kowalski J, Becker DW, Doll J, et al. PET imaging of somatostatin receptors using [68GA] DOTA-D-Phe1-Tyr3-octreotide: first results in patients with meningiomas. *J Nucl Med* 2001; **42**: 1053–6.
59. Thorwarth D, Muller AC, Pfannenberg C, Beyer T. Combined PET/MR imaging using (68)Ga-DOTATOC for radiotherapy treatment planning in meningioma patients. *Recent Results Cancer Res* 2013; **194**: 425–39. doi: 10.1007/978-3-642-27994-2_23
60. Langer DL, van der Kwast TH, Evans AJ, Trachtenberg J, Wilson BC, Haider MA. Prostate cancer detection with multi-parametric MRI: logistic regression analysis of quantitative T2, diffusion-weighted imaging, and dynamic contrast-enhanced MRI. *J Magn Reson Imaging* 2009; **30**: 327–34. doi: 10.1002/jmri.21824
61. Panebianco V, Barchetti F, Sciarra A, Musio D, Forte V, Gentile V, et al. Prostate cancer recurrence after radical prostatectomy: the role of 3-T diffusion imaging in multiparametric magnetic resonance imaging. *Eur Radiol* 2013; **23**: 1745–52. doi: 10.1007/s00330-013-2768-3
62. Drzezga A, Souvatzoglou M, Eiber M, Beer AJ, Furst S, Martinez-Moller A, et al. First clinical experience with integrated whole-body PET/MR: comparison to PET/CT in patients with oncologic diagnoses. *J Nucl Med* 2012; **53**: 845–55. doi: 10.2967/jnumed.111.098608
63. Platzek I, Beuthien-Baumann B, Langner J, Popp M, Schramm G, Ordemann R, et al. PET/MR for therapy response evaluation in malignant lymphoma: initial experience. *MAGMA* 2013; **26**: 49–55. doi: 10.1007/s10334-012-0342-7
64. Quick HH, von Gall C, Zeilinger M, Wiesmuller M, Braun H, Ziegler S, et al. Integrated whole-body PET/MR hybrid imaging: clinical experience. *Invest Radiol* 2013; **48**: 280–9. doi: 10.1097/RLI.0b013e3182845a08
65. Schwenzer NF, Pfannenberg C, Reischl G, Werner MK, Schmidt H. Application of MR/PET in oncologic imaging. [In German.] *Rofo*. 2012; **184**: 780–7. doi: 10.1055/s-0031-1299334
66. Hirsch FW, Sattler B, Sorge I, Kurch L, Viehweger A, Ritter L, et al. PET/MR in children. Initial clinical experience in paediatric oncology using an integrated PET/MR scanner. *Pediatr Radiol* 2013; **43**: 860–75. doi: 10.1007/s00247-012-2570-4
67. Tryggestad E, Flammang A, Han-Oh S, Hales R, Herman J, McNutt T, et al. Respiration-based sorting of dynamic MRI to derive representative 4D-MRI for radiotherapy planning. *Med Phys* 2013; **40**: 051909. doi: 10.1118/1.4800808
68. Schwenzer NF, Schraml C, Muller M, Brendle C, Sauter A, Spengler W, et al. Pulmonary lesion assessment: comparison of whole-body hybrid MR/PET and PET/CT imaging–pilot study. *Radiology* 2012; **264**: 551–8. doi: 10.1148/radiol.12111942
69. Chandarana H, Heacock L, Rakheja R, Demello LR, Bonavita J, Block TK, et al. Pulmonary nodules in patients with primary malignancy: comparison of hybrid PET/MR and PET/CT imaging. *Radiology* 2013; **268**: 874–81. doi: 10.1148/radiol.13130620
70. Ratib O, Beyer T. Whole-body hybrid PET/MRI: ready for clinical use? *Eur J Nucl Med Mol Imaging* 2011; **38**: 992–5. doi: 10.1007/s00259-011-1790-4
71. Kwee TC, Takahara T, Vermoolen MA, Bierings MB, Mali WP, Nievelstein RA. Whole-body diffusion-weighted imaging for staging malignant lymphoma in children. *Pediatr Radiol* 2010; **40**: 1592–602; quiz 720–1. doi: 10.1007/s00247-010-1775-7
72. Baba S, Abe K, Isoda T, Maruoka Y, Sasaki M, Honda H. Impact of FDG-PET/CT in the management of lymphoma. *Ann Nucl Med* 2011; **25**: 701–16. doi: 10.1007/s12149-011-0549-0
73. Hegde JV, Mulkern RV, Panych LP, Fennessy FM, Fedorov A, Maier SE, et al. Multiparametric MRI of prostate cancer: an update on state-of-the-art techniques and their performance in detecting and localizing prostate cancer. *J Magn Reson Imaging* 2013; **37**: 1035–54. doi: 10.1002/jmri.23860
74. Shukla-Dave A, Hricak H. Role of MRI in prostate cancer detection. *NMR Biomed* Mar 2013. Epub ahead of print. doi: 10.1002/nbm.2934
75. Beheshti M, Haim S, Zakavi R, Steinmair M, Waldenberger P, Kunit T, et al. Impact of 18F-choline PET/CT in prostate cancer patients with biochemical recurrence: influence of androgen deprivation therapy and correlation with PSA kinetics. *J Nucl Med* 2013; **54**: 833–40. doi: 10.2967/jnumed.112.110148
76. Quentin M, Schimmöller L, Arsov C, Rabenalt R, Antoch G, Albers P, et al. Increased signal intensity of prostate lesions on high b-value diffusion-weighted images as a predictive sign of malignancy. *Eur Radiol* Aug 2013. Epub ahead of print. doi: 10.1007/s00330-013-2999-3
77. Platzek I, Beuthien-Baumann B, Schneider M, Gudziol V, Langner J, Schramm G, et al. PET/MRI in head and neck cancer: initial experience. *Eur J Nucl Med Mol Imaging* 2013; **40**: 6–11. doi: 10.1007/s00259-012-2248-z
78. Ambrosini V, Tomassetti P, Franchi R, Fanti S. Imaging of NETs with PET radiopharmaceuticals. *Q J Nucl Med Mol Imaging* 2010; **54**: 16–23.
79. Kantorová I, Lipská L, Bêlohlávek O, Visokai V, Trubaĉ M, Schneiderová M. Routine (18)F-FDG PET preoperative staging of colorectal cancer: comparison with

conventional staging and its impact on treatment decision making. *J Nucl Med* 2003; **44**: 1784–8.

80. Halefoglu AM, Atasoy ST, Sakiz D, Baykan A. Accuracy of thin-section magnetic resonance imaging with a pelvic phased-array coil in the local staging of rectal cancer. *J Comput Assist Tomogr* 2013; **37**: 58–64. doi: 10.1097/RCT.0b013e3182772ec5
81. Ruers TJ, Langenhoff BS, Neeleman N, Jager GJ, Strijk S, Wobbes T, et al. Value of positron emission tomography with [F-18] fluorodeoxyglucose in patients with colorectal liver metastases: a prospective study. *J Clin Oncol* 2002; **20**: 388–95.
82. Yong TW, Yuan ZZ, Jun Z, Lin Z, He WZ, Juanqi Z. Sensitivity of PET/MR images in liver metastases from colorectal carcinoma. *Hell J Nucl Med* 2011; **14**: 264–8.
83. Dodge JE, Covens AL, Lacchetti C, Elit LM, Le T, Devries-Aboud M, et al; Gynecology Cancer Disease Site Group. Management of a suspicious adnexal mass: a clinical practice guideline. *Curr Oncol* 2012; **19**: e244–57. doi: 10.3747/co.19.980
84. Brunetti J. PET/CT in gynecologic malignancies. *Radiol Clin North Am* 2013; **51**: 895–911. doi: 10.1016/j.rcl.2013.05.006
85. Castellucci P, Perrone AM, Picchio M, Ghi T, Farsad M, Nanni C, et al. Diagnostic accuracy of 18F-FDG PET/CT in characterizing ovarian lesions and staging ovarian cancer: correlation with transvaginal ultrasonography, computed tomography, and histology. *Nucl Med Commun* 2007; **28**: 589–95. doi: 10.1097/MNM.0b013e3281afa256
86. Kitajima K, Murakami K, Yamasaki E, Kaji Y, Fukasawa I, Inaba N, et al. Diagnostic accuracy of integrated FDG-PET/contrast-enhanced CT in staging ovarian cancer: comparison with enhanced CT. *Eur J Nucl Med Mol Imaging* 2008; **35**: 1912–20. doi: 10.1007/s00259-008-0890-2
87. Sala E, Priest AN, Kataoka M, Graves MJ, McLean MA, Joubert I, et al. Apparent diffusion coefficient and vascular signal fraction measurements with magnetic resonance imaging: feasibility in metastatic ovarian cancer at 3 Tesla: technical development. *Eur Radiol* 2010; **20**: 491–6. doi: 10.1007/s00330-009-1543-y
88. Kinner S, Maderwald S, Albert J, Parohl N, Corot C, Robert P, et al. Comparison of two different iron oxide-based contrast agents for discrimination of benign and malignant lymph nodes. *Invest Radiol* 2012; **47**: 511–15. doi: 10.1097/RLI.0b013e3182587744.
89. Vanel D, Guinebretiere JM, Missenard G, Bonvalot S, Le Cesne A. Indeterminate bone lesion: the diagnosis. *Cancer Imaging* 2002; **2**: 99–100. doi: 10.1102/1470-7330.2002.0011
90. Tateishi U, Yamaguchi U, Seki K, Terauchi T, Arai Y, Kim EE. Bone and soft-tissue sarcoma: preoperative staging with fluorine 18 fluorodeoxyglucose PET/CT and conventional imaging. *Radiology* 2007; **245**: 839–47. doi: 10.1148/radiol.2453061538
91. Gerth HU, Juergens KU, Dirksen U, Gerss J, Schober O, Franzius C. Significant benefit of multimodal imaging: PET/CT compared with PET alone in staging and follow-up of patients with Ewing tumors. *J Nucl Med* 2007; **48**: 1932–1939. doi: 10.2967/jnumed.107.045286
92. Uhl M, Saueressig U, van Buiren M, Kontny U, Niemeyer C, Köhler G, et al. Osteosarcoma: preliminary results of in vivo assessment of tumor necrosis after chemotherapy with diffusion- and perfusion-weighted magnetic resonance imaging. *Invest Radiol* 2006; **41**: 618–23. doi: 10.1097/01.rli.0000225398.17315.68
93. Anagnostopoulos C, Georgakopoulos A, Pianou N, Nekolla SG. Assessment of myocardial perfusion and viability by positron emission tomography. *Int J Cardiol* 2013; **167**: 1737–49. doi: 10.1016/j.ijcard.2012.12.009
94. von Knobelsdorff-Brenkenhoff F, Schulz-Menger J. Cardiovascular magnetic resonance imaging in ischemic heart disease. *J Magn Reson Imaging* 2012; **36**: 20–38. doi: 10.1002/jmri.23580
95. Shapiro BP, Mergo PJ, Austin CO, Kantor B, Gerber TC. Assessing the available techniques for testing myocardial viability: what does the future hold? *Future Cardiol* 2012; **8**: 819–36. doi: 10.2217/fca.12.59
96. Ingkanisorn WP, Rhoads KL, Aletras AH, Kellman P, Arai AE. Gadolinium delayed enhancement cardiovascular magnetic resonance correlates with clinical measures of myocardial infarction. *J Am Coll Cardiol* 2004; **43**: 2253–9. doi: 10.1016/j.jacc.2004.02.046
97. von Schulthess GK, Kuhn FP, Kaufmann P, Veit-Haibach P. Clinical positron emission tomography/magnetic resonance imaging applications. *Semin Nucl Med* 2013; **43**: 3–10. doi: 10.1053/j.semnuclmed.2012.08.005
98. Lee WW, Marinelli B, van der Laan AM, Sena BF, Gorbatov R, Leuschner F, et al. PET/MRI of inflammation in myocardial infarction. *J Am Coll Cardiol* 2012; **59**: 153–63. doi: 10.1016/j.jacc.2011.08.066
99. Stacy MR, Maxfield MW, Sinusas AJ. Targeted molecular imaging of angiogenesis in PET and SPECT: a review. *Yale J Biol Med* 2012; **85**: 75–86.
100. Sasano T, Abraham MR, Chang KC, Ashikaga H, Mills KJ, Holt DP, et al. Abnormal sympathetic innervation of viable myocardium and the substrate of ventricular tachycardia after myocardial infarction. *J Am Coll Cardiol* 2008; **51**: 2266–75.
101. Flett AS, Sado DM, Quarta G, Mirabel M, Pellerin D, Herrey AS, et al. Diffuse myocardial fibrosis in severe aortic stenosis: an equilibrium contrast cardiovascular magnetic resonance study. *Eur Heart J Cardiovasc Imaging* 2012; **13**: 819–26.
102. Banypersad SM, Sado DM, Flett AS, Gibbs SD, Pinney JH, Maestrini V, et al. Quantification of myocardial extracellular volume fraction in systemic AL amyloidosis: an equilibrium contrast cardiovascular magnetic resonance study. *Circ Cardiovasc Imaging* 2013; **6**: 34–9.
103. Glaudemans AW, Quintero AM, Signore A. PET/MRI in infectious and inflammatory diseases: will it be a useful improvement? *Eur J Nucl Med Mol Imaging* 2012; **39**: 745–9. doi: 10.1007/s00259-012-2060-9
104. Satomi T, Ogawa M, Mori I, Ishino S, Kubo K, Magata Y, et al. Comparison of contrast agents for atherosclerosis imaging using cultured macrophages: FDG versus ultrasmall superparamagnetic iron oxide. *J Nucl Med* 2013; **54**: 999–1004.
105. Millon A, Dickson SD, Klink A, Izquierdo-Garcia D, Bini J, Lancelot E, et al. Monitoring plaque inflammation in atherosclerotic rabbits with an iron oxide (P904) and (18)F-FDG using a combined PET/MR scanner. *Atherosclerosis* 2013; **228**: 339–45. doi: 10.1016/j.atherosclerosis.2013.03.019
106. Glaus C, Rossin R, Welch MJ, Bao G. In vivo evaluation of (64)Cu-labeled magnetic nanoparticles as a dual-modality PET/MR imaging agent. *Bioconjug Chem* 2010; **21**: 715–22. doi: 10.1021/bc900511j
107. Jarrett BR, Correa C, Ma KL, Louie AY. In vivo mapping of vascular inflammation using multimodal imaging. *PLoS One* 2010; **5**: e13254. doi: 10.1371/journal.pone.0013254
108. Grand DJ, Beland M, Harris A. Magnetic resonance enterography. *Radiol Clin North Am* 2013; **51**: 99–112. doi: 10.1016/j.rcl.2012.09.007
109. Costa-Silva L, Brandao AC. MR enterography for the assessment of small bowel diseases. *Magn Reson Imaging Clin N Am* 2013; **21**: 365–83. doi: 10.1016/j.mric.2013.01.005